

# **Comparative Structural Seismic Performance of a 10-Story Commercial Building Using Lightweight Precast Concrete Panels and Lightweight Brick Wall Systems**

Naisha Elvira Tanjung, Ivan Imanuel\*, Ika Bali

Department of Civil Engineering, President University, Cikarang, Indonesia

Received 07 October 2025; received in revised form 13 October 2025; accepted 15 October 2025

## **Abstract**

This study presents a comparative seismic performance analysis of a 10-story commercial building in North Jakarta, an area characterized by high seismicity and challenging geotechnical conditions. Two identical structural models were analyzed using ETABS v2022: one using a lightweight precast concrete panel system (JOE Green X3) and the other using a conventional Autoclaved Aerated Concrete (AAC) lightweight brick system. The aim is to compare the seismic structural performance of the analysis, based on the response spectrum method in accordance with SNI 1726:2019, revealed that the precast concrete panel system, was 14.4% lighter than the AAC lightweight bricks system when accounting for its full installed weight, including plaster and bracing columns. It resulted in a shorter fundamental period (0.412 s) compared to 0.453 s of the AAC lightweight brick system. However, the seismic base shear forces are nearly identical due to compensating effects in the site-specific response spectrum. Although both systems meet the deflection limits mandated by regulations, their performance is direction-dependent. This study concludes that the substantial reduction in total mass of the precast panel system provides a shorter vibration period but comparable seismic performance to the AAC lightweight brick system.

**Keywords:** seismic performance, inter-story drift, lightweight precast concrete panels, JOE Green X3, AAC lightweight bricks

## **1. Introduction**

The construction of high-rise buildings in coastal urban areas such as North Jakarta faces dual engineering challenges: high seismic risk and severe geotechnical constraints, particularly the phenomenon of land subsidence [1-2]. These conditions require a design strategy that focuses not only on structural efficiency but also on minimizing permanent loads to ensure safety and long-term service life. In this context, reducing structural mass is no longer merely an economic goal, but a fundamental engineering requirement [3-6].

Autoclaved Aerated Concrete (AAC) has long been utilized as a lightweight wall material to reduce seismic mass. However, advances in precast technology have led to the development of lightweight precast concrete panels, offering an alternative system. Lightweight precast concrete panels and lightweight brick or block wall systems have been widely recognized for their ability to enhance seismic performance by reducing the overall structural mass and thus lowering the inertial forces generated during earthquakes. For instance, research on prefabricated lightweight concrete-polystyrene composite wall panels demonstrated that these systems effectively reduce dead loads while improving lateral resistance.

---

\* Corresponding author. E-mail address: ivan.immanuel@president.ac.id, ivan.immanuel@yahoo.com

Tel.: +62(81322847163)

Similarly, lightweight composite exterior wallboards in steel frames have been found to enhance seismic behavior by minimizing mass and stiffness degradation [7]. Comparative studies also confirmed that lighter infill materials such as lightweight precast concrete, autoclaved aerated concrete (AAC), and fly ash bricks attract smaller base shear forces than conventional clay brick walls [8].

From a dynamic perspective, a greater structural mass tends to increase the fundamental period of vibration [9] and amplify the seismic inertial force. Conversely, wall systems with higher rigidity, such as precast concrete panels, can shorten the vibration period, produce a stiffer structural response but potentially attract higher seismic forces depending on the acceleration spectrum [3]. This interaction between mass and stiffness directly influences the base shear experienced by a structure. According to the earthquake design principles in SNI 1726:2019, the base shear force ( $V$ ) is expressed as the product of the effective seismic mass ( $W$ ) and the seismic response coefficient ( $C_s$ ) [4].

Despite extensive research on the seismic performance of individual lightweight wall systems, there remains limited comparative analysis of how different lightweight materials such as precast concrete panels and lightweight brick affect the overall seismic response of multi-story buildings. This paper presents the comparison of the structural response to seismic loading between the use of lightweight precast concrete panel system and the AAC lightweight brick wall system in a 10-story building located in North Jakarta. The research aims to compare the seismic performance on three key indicators of structural performance: vibration period, base shear force, and inter-story drift.

## 2. Method and Loading

This study uses a quantitative methodology with a comparative study design, using numerical techniques and ETABS to evaluate structural performance. The research design involves a comparative analysis of three-dimensional (3D) structural models that are identical in all aspects except for their non-structural infill wall systems. The study methodology, from data collection to conclusions, is illustrated in Fig. 1.

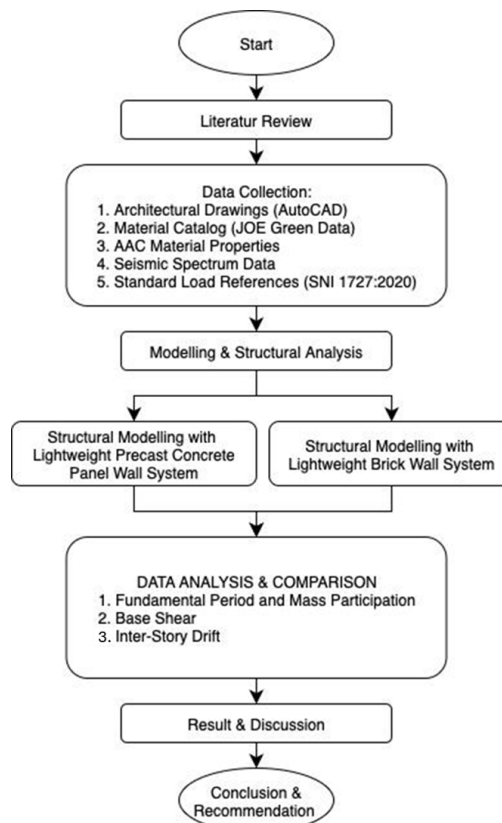


Fig. 1 Study methodology

2.1 Modeling scenarios

Two structural models of a 10-story building were developed using ETABS to evaluate the influence of different wall systems. The first model represents the conventional AAC lightweight brick system (Scenario A), in which the wall is modeled as a masonry membrane element with a material density calibrated to reflect the combined weight of AAC blocks and plaster. To account for the additional weight of the practically integrated columns, a uniform shell load is also applied to the element. The second model corresponds to the lightweight precast concrete panel system (Scenario B), where the wall is defined as a masonry membrane element with material density adjusted to represent the total installed weight of the JOE Green Panel X3 system, including both the panel and the integrated skim coat finish.

2.2 Site conditions and seismic parameters

The reference structure for this analysis is a 10-story commercial building located in Pluit, North Jakarta. Based on SNI 1726:2019 regulations [10], the location is classified as SE Site Class (Soft Soil), which tends to amplify seismic waves. The seismic parameters for the analysis were determined from the official Indonesian government portal, [rsa.ciptakarya.pu.go.id](http://rsa.ciptakarya.pu.go.id), [11] for the specific project location. The resulting design response spectrum is shown in Fig. 2 and Fig. 3.

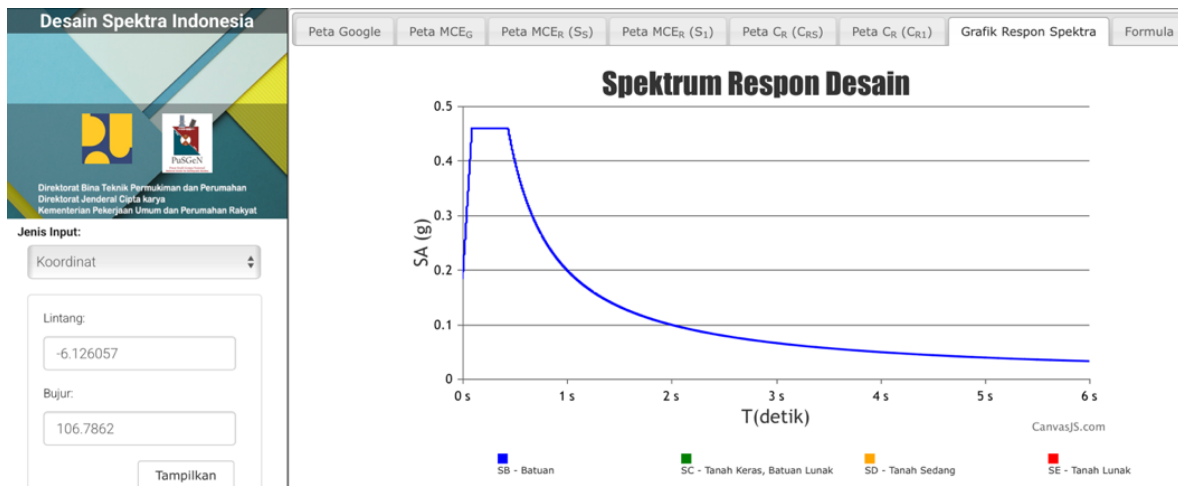


Fig. 2 Design response spectrum for the Pluit area



Fig. 3 Response spectrum data for the Pluit area

The combination of the base rock acceleration and site coefficients yields design spectral acceleration parameters of  $S_{ds}=0.65$  and  $S_{d1}=0.63$ . These values place the structure in Seismic Design Category 'D' (see Table 1), indicating a high level of earthquake hazard and requiring the use of a special seismic force-resisting system. This data forms the basis for the response spectrum analysis in ETABS.

Table 1 Seismic design parameters for the project site

Seismic parameter	Value	Description / formula	Reference (SNI 1726:2019)
Risk category	II	General buildings: shopping centers, offices, shops	Table 3
Earthquake importance factor ( $I_e$ )	1.0	Based on risk category II $\rightarrow I_e = 1$	Table 4
Site soil classification	SE	Soft soil ( $V_s$ 128-175 m/s, NSPT < 15)	Table 5
$S_s$ (MCEr)	0.7623 g	Spectral response acceleration at short period (MCEr)	$S_s$ map (Spectral Indonesia)
$S_1$ (MCEr)	0.3766 g	Spectral response acceleration at 1-second period (MCEr)	$S_1$ map (Spectral Indonesia)
PGA (MCEr)	0.3645 g	Peak Ground Acceleration from MCEr	PGA map
$F_a$ (site coefficient, 0.2 s)	1,279	From interpolation of Table $F_a$ for site class SE and $S_s$	Table 6
$F_v$ (site coefficient, 1 s)	2.5093	From interpolation of Table $F_v$ for site class SE and $S_1$	Table 7
SMS (adjusted $S_s$ )	0.975	$SMS = F_a \times S_s = 1.2790 \times 0.7623$	Clause 6.2
SM1 (adjusted $S_1$ )	0.945	$SM1 = F_v \times S_1 = 2.5093 \times 0.3766$	Clause 6.2
$S_{ds}$ (design, 0.2 s)	0.65	$S_{ds} = (2/3) \times SMS = (2/3) \times 0.975$	Clause 6.3
$S_{d1}$ (design, 1 s)	0.63	$S_{d1} = (2/3) \times SM1 = (2/3) \times 0.945$	Clause 6.3
Seismic design category	D	Since $S_{ds} = 0.65 > 0.5$ and $S_{d1} = 0.63 > 0.2$	Tables 8 & 9, Clause 6.5

### 2.3 Structural system and numerical modeling

The main lateral force-resisting system for the structure was defined as a Special Moment-Resisting Frame (SMRF) made of reinforced concrete. This system was chosen in accordance with SNI 1726:2019 requirements for Seismic Design Category 'D', which mandates a ductile structural system. The following design parameters were adopted: a Response Modification Factor ( $R$ ) of 8, a System Overstrength Factor ( $\Omega$ ) of 3, and a Deflection Amplification Factor ( $C_d$ ) of 5.5.

Numerical analysis was performed using ETABS v2022 software to create two identical three-dimensional models. Seismic performance was evaluated using the response spectrum analysis method with a design spectrum specific to the Pluit location. All loading standards, including dead load ( $D$ ), live load ( $L$ ), and earthquake load ( $E$ ), refer to SNI 1727:2020 [12-13] and SNI 1726:2019 [10]. In both scenarios, the infill walls were modeled as Membrane elements with a stiffness modification factor of 0.25 applied to their membrane properties ( $f_{11}$ ,  $f_{22}$ ,  $f_{12}$ ) to simulate realistic post-cracking conditions in brittle non-structural elements.

### 2.4 Infill wall systems and modeling parameters

The core of this analysis is a comparison of two infill wall systems, defined based on their complete, installed construction systems. The fundamental differences between these two systems are summarized in

Table 2. To provide a clear representation of how each wall system was defined in the analysis, the material properties were calibrated in ETABS. Fig. 4 shows the input data for the lightweight precast concrete panel, where the material density was set to 998 kg/m<sup>3</sup> to reflect its total installed weight. **Error! Reference source not found.** shows the input data for the AAC lightweight brick wall, where the density was set to 1338 kg/m<sup>3</sup> to account for the weight of the block and plaster, with the weight of practical columns applied separately.

Table 2 Comparison of wall system specifications and installed weight

Property	AAC lightweight brick wall	Lightweight precast concrete panel (Joe Green panel X3)
Weight without plaster (kg/m <sup>2</sup> )	70	96
Compressive strength (MPa)	3 – 4	> 15
Typical thickness (mm)	100	100
Plaster (kg/m <sup>2</sup> ) $w=\gamma \times t \times 2(\text{side})$	$2000 \times 0.015 \times 2 = 60$	None
Skim coat (kg/m <sup>2</sup> ) $w=\gamma \times t$	$1900 \times 0.002 \approx 3.8$	$0.002 \times 1,900 \approx 3.8$
Estimated installed weight (kg/m <sup>2</sup> ) (Winst)	$(133.8 \text{ kg/m}^2 \times 9.81 \text{ m/s}) / 1000 = 1.31 \text{ kN/m}^2$	$(99.8 \text{ kg/m}^2 \times 9.81 \text{ m/s}) / 1000 = 0.979 \text{ kN/m}^2$
Column practice $w=A \times \gamma$	$A=0.15 \times 0.15 = 0.0225 \text{ m}^2$	None
	$w=0.0225 \text{ m}^2 \times 24 \text{ kN/m}^3 = 0.54 \text{ kN/m}$	

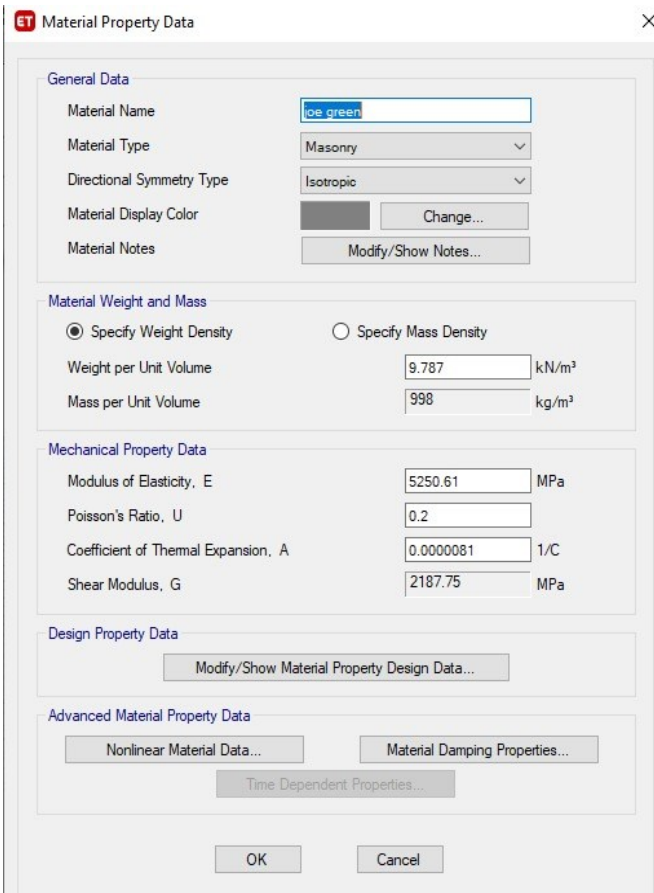


Fig. 4 Input data for lightweight precast concrete panel model

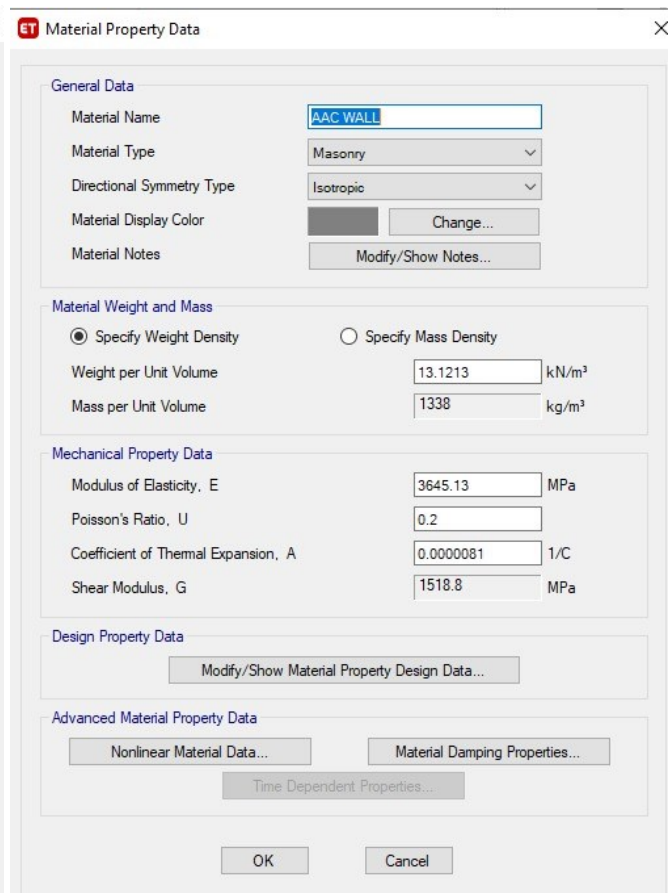


Fig. 5 Input data for AAC lightweight brick wall model

## 2.5 Loading criteria

The loading criteria were based on relevant national standards. The dead load includes the structure's self-weight (calculated automatically by ETABS) and the superimposed dead load (SDL). The SDL for typical floor slabs was calculated at 1.2 kN/m<sup>2</sup>, as detailed in Table 3. For the roof area, the SDL is greater due to the waterproofing layer, with a total of 1.55 kN/m<sup>2</sup>, as shown in Table 4. The load of the elevator machine room is calculated as an additional dead load, with values varying as shown in

Table 5.

Table 3 Superimposed dead load for typical slabs

Superimposed dead load (Typical slab)				
Load components	Thickness (m)	Specific gravity (kN/m <sup>3</sup> )	Load (kN/m <sup>2</sup> )	Reference source
Ceramics & adhesives	0.01	-	0.24	Typical producer data
Screed	0.03	22	0.66	SNI 1727:2020 [11] & PPURG 1987 [12]
Ceiling + frame	-	-	0.2	PPURG 1987 [12]
MEP installation	-	-	0.1	General engineering practices
Total			1.2	

Table 4 Superimposed dead load for roof slabs

Superimposed load (Roof slab)				
Load components	Thickness (m)	Specific gravity (kN/m <sup>3</sup> )	Load (kN/m <sup>2</sup> )	Reference source
Waterproofing layer	Double-layer membrane	-	0.2	Typical producer data
Screed	0.05	22	1.1	SNI 1727:2020 [11] & PPURG 1987 [12]
Ceiling + frame	-	-	0.2	PPURG 1987 [12]
MEP installation	-	-	0.05	General engineering practices
Total			1.55	

Table 5 Superimposed dead load for elevator machine room

Machine room load					
Lift	Length (m)	Width (m)	Area (m <sup>2</sup> ) = W×L	Uniform load q (kN/m <sup>2</sup> )	P = q × A (kN)
A1	2.7	2.1	5.67	4.8	27.216
A2	2.7	2.1	5.67	4.8	27.216
A3	2.7	2.1	5.67	4.8	27.216
A4	3	2.6	7.8	4.8	37.44
A5	3	2.6	7.8	4.8	37.44
A6	3.25	3.2	10.4	4.8	49.92
A7	3.25	2.5	8.125	4.8	39

The live load was determined based on the function of each floor in accordance with SNI 1727:2020. Rain, wind, and earthquake loads were also applied in accordance with applicable standards. The first and fifth floors (LT1 and LT5) function as parking areas, each designed with a live load of 3.92 kN/m<sup>2</sup>. The second, third, and fourth floors (LT2–LT4) serve as supermarket areas, where higher occupancy and merchandise loads are expected; therefore, a live load of 4.79 kN/m<sup>2</sup> is applied to each of these levels. The upper commercial levels (LT7–LT9) are designated as office spaces, which typically impose moderate live loads; accordingly, a value of 2.40 kN/m<sup>2</sup> is adopted for these floors. At the top of the structure, the roof slab (LT10) carries a nominal live load of 0.96 kN/m<sup>2</sup> to represent maintenance and environmental service access. Additionally, a separate roof area is designated for a gym facility (LT10 R. Gym), which requires a higher live load of 4.79 kN/m<sup>2</sup> to account for dynamic occupant activity and exercise equipment.

### 3. Results and Discussion

A structural comparison analysis was performed on the 3D model visualized in Fig. 5. This section presents the numerical results of both models, focusing on the comparison of three key seismic performance parameters.

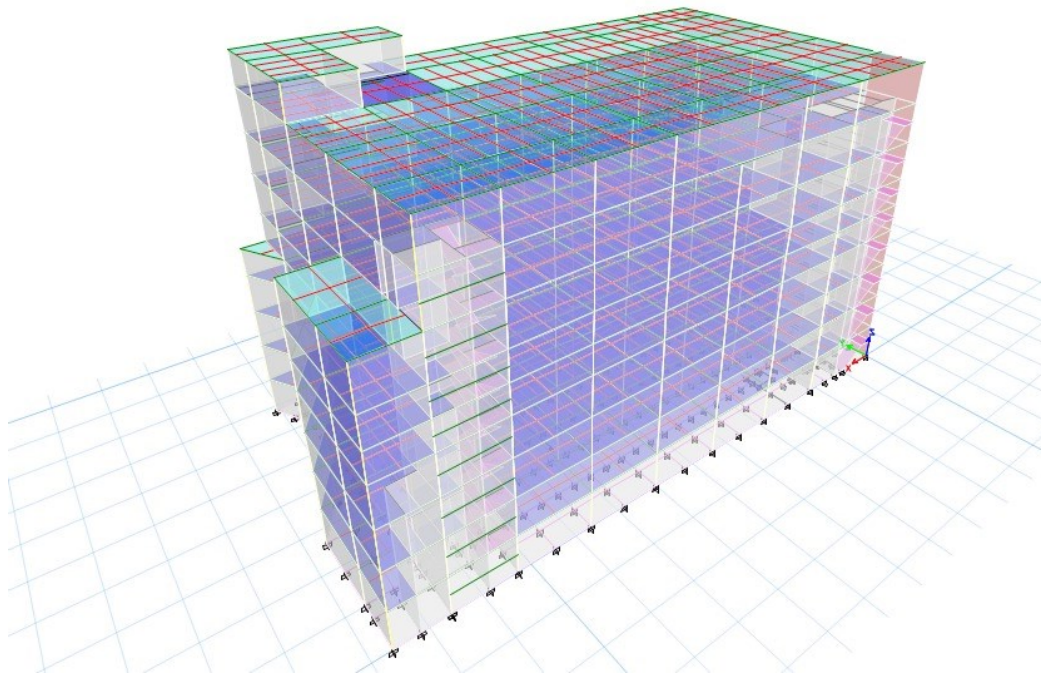


Fig. 5 structural modelling in ETABS

#### 3.1 Total structural mass and geotechnical implications

The analysis began with an evaluation of the total mass of each model, which was verified by summing the vertical base reactions due to dead load. The results, summarized in Table , showed that the model with Precast Concrete Panel was significantly lighter.

Table 6 Total structural mass comparison

Parameter	AAC lightweight brick model	Lightweight precast concrete panel model	Difference
Total vertical reaction (Dead load FZ)	308,986.06 kN	270,181.04 kN	38,804.95 kN
Relative mass difference	Reference	-14.4%	-

The determining factor here is the "installed system weight"; the need for thick plastering and reinforced concrete columns in the AAC system adds substantial dead weight, which outweighs the advantages of the base material's lower density. This 14.4% change in total mass has critical geotechnical implications, especially for the project site in Pluit, which is known for its soft soil conditions and susceptibility to land subsidence. The lighter permanent dead load of the Precast Panel system directly reduces long-term pressure on the foundation system, which can lead to a more efficient foundation design and increase the structure's resilience to differential settlement.

### 3.2 Fundamental vibration period

Fundamental dynamic characteristics, particularly the natural vibration period ( $T$ ), determine how a structure responds to seismic shocks. The results, shown in Table , indicate a key finding. The model using AAC walls has a longer fundamental period ( $T=0.453$  s) than the model using precast panels ( $T=0.412$  s). This indicates that, overall, the AAC system is more flexible (less rigid). This highlights the complex relationship between mass and stiffness; although the plaster and columns in the AAC system provide additional stiffness, this effect is dominated by the significant increase in total mass, which is the main factor causing the longer vibration period.

Table 7 Comparison of structural dynamic characteristics

Parameter	AAC lightweight brick model	Lightweight precast concrete panel model	Implication
Fundamental period ( $T$ )	0.453 s	0.412 s	AAC model is more flexible (less rigid).

### 3.3 Base shear analysis

The base shear force is the total seismic lateral force acting on the base of the structure. One of the most interesting findings of this study, shown in Table , is that the base shear for both models is nearly identical.

Table 8 Comparison of maximum basic shear force in the x direction

Model	Output case	Base shear $V_x$ (kN)
AAC lightweight brick model	Eq Sx	2,976.53 kN
Lightweight precast concrete panel model	Eq Sx	2,987.45 kN

This phenomenon, with a difference of less than 0.4%, can be attributed to the complex interaction among mass, period, and the site-specific design response spectrum. Essentially, a mutually compensating exchange occurs between the two systems. The AAC lightweight brick model possesses a significantly higher effective seismic mass ( $W$ ) of approximately 14.4%, which would typically increase the base shear force. However, its longer fundamental period ( $T = 0.453$  s) positions within a region of the response spectrum characterized by a slightly lower seismic response coefficient ( $C_s$ ). In contrast, the lightweight precast concrete panel model has a lighter effective seismic mass but a shorter fundamental period ( $T = 0.412$  s), placing it within a region of the spectrum associated with a relatively higher  $C_s$  value.

As a result, the higher mass of the AAC model is effectively counterbalanced by a lower  $C_s$ , while the lighter mass of the precast model is offset by a higher  $C_s$ . Consequently, both systems experience nearly identical total seismic forces, indicating that, in terms of overall force demand, neither system demonstrates a distinct advantage.

### 3.4 Inter-story drift

Inter-story drift is a critical seismic performance indicator as it relates directly to non-structural damage and P-Delta stability. While both models easily meet the 86 mm drift limit set by SNI 1726:2019, the comparative analysis reveals complex, direction-dependent results, as shown in Table 6.

Table 6 Inspection of maximum inter-floor deviation compliance

Direction	Model	Maximum drift (mm)	Story location	SNI limit (mm)	Status
X-axis	AAC lightweight brick model	1.03	9th Floor	86	Complies
X-axis	Lightweight precast concrete panel model	1.60	4th Floor	86	Complies
Y-axis	AAC lightweight brick model	1.76	2nd Floor	86	Complies
Y-axis	Lightweight precast concrete panel model	1.32	4th Floor	86	Complies

The performance differences between the two systems are notable. In the X-direction, the AAC lightweight brick model demonstrates superior performance, with a maximum deviation approximately 36% lower than that of the precast panel model. This suggests that, for responses in this direction, the additional stiffness provided by the plaster and column elements in the AAC system is more influential than the effect of its added mass.

Conversely, in the Y-direction, the AAC model exhibits a maximum deviation approximately 33% higher than the precast panel model. In this case, the substantial increase in the total mass of the AAC system becomes the dominant factor, leading to greater deviation despite the presence of stiffening components. These findings emphasize that drift performance cannot be generalized, as it strongly depends on the interaction between the mass and stiffness of the wall system components and how these factors influence the building's response in each orthogonal direction.

## 4. Conclusions

Based on the results of the comparative analysis and discussion, several key findings can be highlighted. The lightweight precast concrete panel model exhibits a lighter total mass than the AAC lightweight brick model, resulting in a shorter fundamental vibration period ( $T = 0.412$  s) and a stiffer structural response. Despite the significant difference in mass, both models experience nearly identical total seismic base shear forces, with a discrepancy of less than 0.4%. This phenomenon occurs because the reduced mass of the precast system is compensated by a higher seismic response coefficient associated with its shorter natural period.

Although both systems meet the safety criteria specified in SNI 1726:2019, their inter-story drift performance varies depending on the direction. The precast system performs 33% better in controlling drift in the Y-direction, whereas the AAC system performs 36% better in the X-direction. Overall, despite its primary advantage in substantially reducing total structural mass and fundamental vibration period, the lightweight precast concrete panel system demonstrates nearly equivalent seismic performance to the AAC lightweight brick wall system in terms of base shear and inter-story drift.

## References

- [1] A. Abidin, H. Andreas, D. Gumilar, T. P. Sidiq, and Y. Fukuda, "Land Subsidence in Coastal City of Semarang (Indonesia): Characteristics, Impacts and Causes," *Geomat. Nat. Hazards Risk*, vol. 4, no. 3, pp. 226–240, 2013, doi: 10.1080/19475705.2012.692336.

- [2] H. Andreas, A. Abidin, D. Sarsito, and H. Z. Lubis, "Land Subsidence in Jakarta and Its Relation with Urban Development," *Nat. Hazards*, vol. 59, no. 3, pp. 1753–1771, 2011, doi: 10.1007/s11069-011-9866-9.
- [3] S. Guettala, A. Khelaifia, R. Chebili, and S. Guettala, "Effect of Infill Walls on Seismic Performance of Multi-Story Buildings with Shear Walls," *Asian J. Civ. Eng.*, vol. 25, no. 5, pp. 3989–3999, 2024, doi: 10.1007/s42107-024-01025-9.
- [4] M. R. Shendkar, D. P. N. Kontoni, E. Işık, S. Mandal, P. R. Maiti, and E. Harirchian, "Influence of Masonry Infill on Seismic Design Factors of Reinforced-Concrete Buildings," *Shock Vib.*, vol. 2022, no. 1, 2022, doi: 10.1155/2022/5521162.
- [5] M. I. Ahmed, A. Zafar, R. Alturki, and M. I. Khan, "Optimization and Performance of Expanded Polystyrene Concrete for Sustainable Infill Wall Construction Using Response Surface Methodology," *Sci. Rep.*, vol. 15, no. 1, 2025, doi: 10.1038/s41598-025-07705-z.
- [6] I. Bali, J. Widjajakusuma, G. P. Ng, and R. Tjahjono, "High Early Strength Foamed Concrete Design for Structural Precast Concrete," *IOP Conf. Ser.: Earth Environ. Sci.*, vol. 1195, no. 1, p. 012022, June 2023, doi: 10.1088/1755-1315/1195/1/012022.
- [7] K. Zhao, Z. Fan, Y. Zhang, Y. Xu, and S. Liu, "Experimental Study on Seismic Performance of Prefabricated Monolithic Concrete–Polystyrene Panel Composite Wall Panels," *Buildings*, vol. 14, no. 2, 2024, doi: 10.3390/buildings14020442.
- [8] A. Thakur and K. Senthil, "Seismic Performance of Confined Masonry Walls with Different Infill Materials: A Comparative Study," *Asian J. Civ. Eng.*, vol. 25, pp. 1587–1599, 2024, doi: 10.1007/s42107-023-00863-3.
- [9] S. Wang, G. Zhang, C. Gunasekara, D. Law, Y. Tan, and W. Sun, "A Scientific Review of Recycling Practices and Challenges for Autoclaved Aerated Concrete in Sustainable Construction," *Buildings*, vol. 15, no. 14, 2025, doi: 10.3390/buildings15142453.
- [10] Badan Standardisasi Nasional, SNI 1726:2019 Tata Cara Perencanaan Ketahanan Gempa untuk Struktur Bangunan Gedung dan Nongedung, Jakarta, Indonesia, 2019. (in Indonesian).
- [11] Kementerian PUPR, Desain Spektra Indonesia. [Online]. Available: <https://rsa.ciptakarya.pu.go.id/2021/>. [Accessed: Oct. 7, 2025].
- [12] Badan Standardisasi Nasional, SNI 1727:2020 Beban Desain Minimum dan Kriteria Terkait untuk Bangunan Gedung dan Struktur Lain, Jakarta, Indonesia, 2020. (in Indonesian).
- [13] Departemen PU, Pedoman Perencanaan Pembebanan untuk Rumah dan Gedung, Jakarta: Yayasan Badan Penerbit PU, 1987. (in Indonesian).